

Article

Unlocking Strategic and Critical Raw Materials: Assessment of Zinc and REEs Enrichment in Tailings and Zn-Carbonate in a Historical Mining Area (Montevecchio, SW Sardinia)

Lorenzo Sedda, Giovanni De Giudici , Dario Fancello, Francesca Podda and Stefano Naitza * 

Dipartimento di Scienze Chimiche e Geologiche, Università degli Studi di Cagliari, 09124 Cagliari, Italy; lorenzo.sedda@unica.it (L.S.); gbgiudic@unica.it (G.D.G.); dario.fancello@unica.it (D.F.); fpodda@unica.it (F.P.)

* Correspondence: snaitza@unica.it

Abstract: Mining wastes are often both a potential source of Strategic and Critical Raw Materials (SRMs and CRMs) and a threat to the environment. This study investigated the potential of mining wastes from the Montevecchio district of Sardinia, Italy, as a source of SRMs and CRMs. The tailings from Sanna mine processing plant were characterized by X-ray diffraction, Scanning Electron Microscopy, and Plasma Mass Spectrometry, showing contents of 1.2 wt% of lead, 2.6 wt% of zinc, and about 600 mg/kg of Rare Earth Elements (REEs). White patinas formed in the riverbed, composed by Zn-bearing minerals (hydrozincite and zincite), also contain about 2900 mg/kg of REEs. Characterization of white patinas along the Rio Roia Cani evidenced that their precipitation from water also involves an uptake of Rare Earth Elements, enhancing their contents by an order of magnitude compared with tailings. The process of REEs concentration in Zn-bearing minerals of white patinas is a candidate as a tool for the economic recovery of these elements. These findings suggest that mining wastes from the Montevecchio district could be considered a potential resource for extracting SRMs and CRMs.



Citation: Sedda, L.; De Giudici, G.; Fancello, D.; Podda, F.; Naitza, S. Unlocking Strategic and Critical Raw Materials: Assessment of Zinc and REEs Enrichment in Tailings and Zn-Carbonate in a Historical Mining Area (Montevecchio, SW Sardinia). *Minerals* **2024**, *14*, 3. <https://doi.org/10.3390/min14010003>

Academic Editor: María Ángeles Martín-Lara

Received: 20 October 2023

Revised: 4 December 2023

Accepted: 14 December 2023

Published: 19 December 2023



Copyright: © 2023 by the authors. Licensee MDPI, Basel, Switzerland. This article is an open access article distributed under the terms and conditions of the Creative Commons Attribution (CC BY) license (<https://creativecommons.org/licenses/by/4.0/>).

Keywords: metal recovery; critical raw materials; green economy

1. Introduction

The search for Critical Raw Materials (CRMs) for the energy transition and an ever-greener economy is increasingly important for the European Union in order to secure supplies and reduce dependence on unsafe sources. Since 2011, the EU updates its list of CMRs every three years, now including 35 raw materials of critical and strategic relevance [1]. This prompted the European Commission to support new exploration activities in the old mine districts of the EU members. A specific target of this new research is represented by mining wastes and tailings, whose exploitation may allow the recovery of neglected resources, enhancing at the same time the environmental quality of the involved areas by removing large volumes of contaminated materials [2].

Tailings are different types of waste materials produced by the processing of ore bodies, containing economic metals and minerals, which pose a threat to the environment and various ecosystems. That implies that tailings represent an important source of contamination for the environment for various ecosystems and for the people. A solution could be the re-treatment of these tailings for the extraction of these metals and metalloids if these are contained in economic contents, implicating the removal of a source of contaminations. This solution has several advantages: it allows the recovery of valuable resources that would otherwise have been lost; it reduces the amount of tailings that need to be stored, thus reducing the risk of environmental contamination; and it improves the overall sustainability of the mining sector. Tailings reprocessing must adhere to responsible and sustainable practices, minimizing environmental impact, ensuring worker and community safety, and maintaining cost-effectiveness through market price recovery of metals and

metalloids. An essential phase for the definition of these projects consists in the mapping and characterization of the various mining landfills, to define their volumes, surfaces, and concentrations of raw materials [3–5].

Sardinia was a relevant mining region at the European scale, particularly for the extraction of lead and zinc ores. The Montevecchio district, located in SW Sardinia, was one of Italy's most important mining areas for over a century. Mining activities in the district ended in 1991 [6]. Today, it is one of Sardinia's most historically significant mining sites, featuring architecturally valuable abandoned mining buildings and shafts. Beyond this legacy of industrial archaeology, in Montevecchio there are numerous and very large mining dumps that represent a serious environmental problem on a national scale [7]. At the same time, it is increasingly evident from recent studies and geochemical/environmental characterizations [8,9] that these materials may contain significant amounts of base metals and strategic elements, thus becoming a potentially relevant target for CRM research.

The mining area is located between the municipalities of Arbus and Guspini, in South-western Sardinia (Figure 1). The intense underground mining activity deeply exploited a huge, NE-SW-directed mineralized vein system, producing about 2 million cubic meters of excavations voids and over 2 million cubic meters of mining dumps. Moreover, the processing plants produced over 6 million cubic meters of tailings [10]. The mining activity was focused on the extraction of minerals containing lead, zinc, and silver, but a large set of associated metals (Cu, Ni, Co, Bi, Sb, In, Ga, Ge, etc.) was recovered in the metallurgical cycles. The mine exploited two types of mineralization, sulfide, and oxidated ores, that required two different treatments to be recovered. Accordingly, two different plants were built in the mine area: the eastern plant (named the Principe Tommaso plant) processed the sulfide minerals, and the western plant (named the Sanna plant) processed the oxidate minerals. Thus, very different tailing materials are currently accumulated in the two old plant areas.

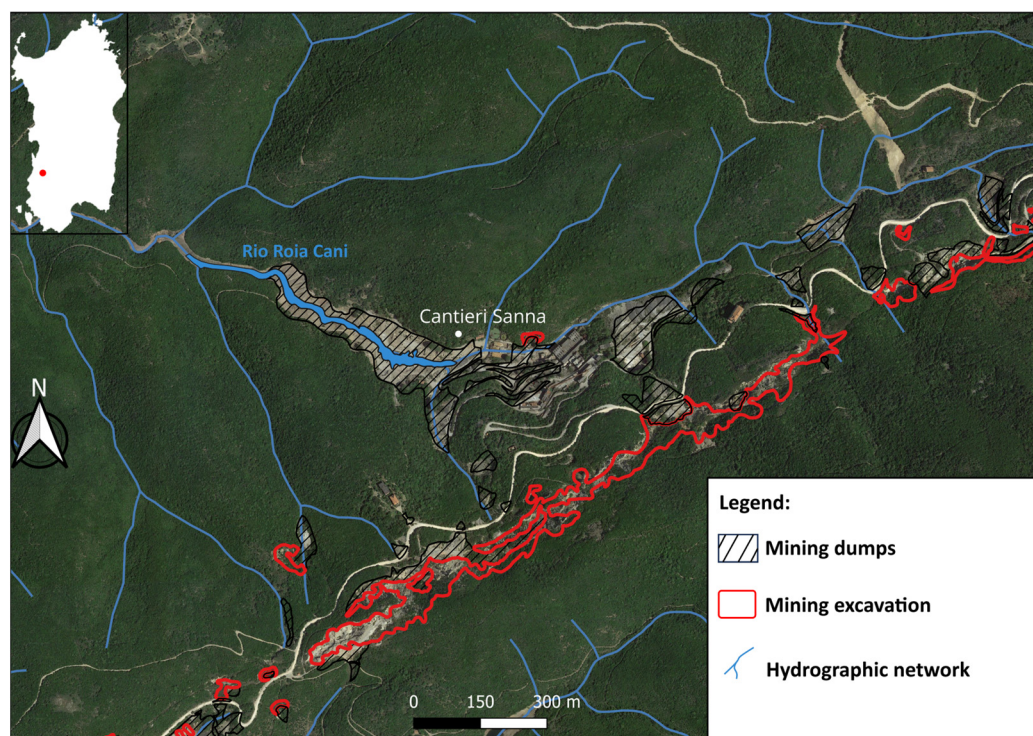


Figure 1. The study area. The main elements related to mining operations (mining dumps and excavation) are evidenced.

This work is focused on the tailings of the Sanna plant, whose composition and current arrangement are a product of the technological evolution of the processing systems for over

a century. In detail, oxidate minerals from the whole Montevecchio district were initially processed in the earlier Sanna-Eleonora plant (1869–1936). The process involved a first hammer-sorting, a second hand-sorting, and finally, a separation using jigs and shaking tables. Starting from 1937 and up to 1980, the ores were treated in the new Sanna plant where minerals were first comminuted by jaw and gyratory crushers, then finely ground by ball mills, and finally enriched by flotation [11]. Both the old and the new plants were set along the valley of the Rio Roia Cani stream, which flows from the mine area towards the west. The resulting tailings, of variable grain size, are now accumulated along the valley and are affected by important erosional phenomena that imply instability of the dumps and produce solid and chemical transport of potentially polluting materials, generating contamination over a large area downstream. Several past studies in the Montevecchio district pointed out that rivers of the area may carry high amounts of metals in solution after having interacted with the mining environments [12–17]. Evidence of the extent of these phenomena are the mineral precipitates (white patinas) that frequently encrust outcropping rocks, pebbles, and sediments at the bottom of the Roia Cani riverbed. They appear analogous to the hydrozincite bio-precipitates induced by bacterial activity, extensively documented in another mining area of the same district (Ingurtosu Mine) along the Rio Naracauli [18,19]. With the dual objective of verifying the possible presence of metals and CRMs in the tailings and the environmental conditions of the area, the study starts from a mineralogical and chemical characterization of the wastes of the Sanna plant but also encompasses some representative minerals of the ore that fed the plant, the Rio Roia Cani waters that directly interact with the wastes, and particularly, the white patinas along the Rio Roia Cani riverbed. Indeed, these latter not only may be considered as markers of the grade of diffusion of pollutants and of their biologically mediated interactions with the natural environment but also may provide interesting information about natural processes of re-concentration of metals and CRMs that may have potential economic implications.

2. Geological Setting

The Montevecchio mine area is located in the external nappe zone (allochthonous Arburese unit) of the Palaeozoic basement of Southwestern Sardinia, close to the contact with the Variscan Foreland (Autochthonous Iglesiente Unit). These low-grade metamorphic units are intruded by the granitoids of the Arbus pluton (304 ± 1 Ma), which determined only moderate thermometamorphic effects in a relatively thin aureola [20].

The geology of the area is dominated by the Upper Cambrian-Lower Ordovician rocks of the Arenarie di San Vito Formation (Arburè tectonic Unit), consisting of fine metasandstones, metasilstones, and metargillites [21]. This sequence is unconformably covered by Middle-Ordovician felsic metavolcanic rocks of rhyolitic-rhyodacitic composition [22,23].

The Palaeozoic rocks are in turn unconformably covered by Tertiary clastic sediments of the Ussana Formation, consisting of conglomerates, breccias, and sandstones with a red-purple clayey-sandstone matrix [21], and by the Oligo-Miocene calc-alkaline sequences of the Monte Arcuentu volcanic complex [23].

3. The Montevecchio Ore Deposits

The large Montevecchio hydrothermal vein system [6] consists of a series of mineralized veins that follow with a “pinch-and-swell” attitude the northern contact of the Arbus pluton for a length of over ten kilometres in a NE-SW direction (Figure 2). The vein field has held great economic importance in the past, having been among the largest in Western Europe; the thickness of the mineralized veins could reach 25–30 m at some points. From east to west, the veins are called: Sant’Antonio, Piccalinna, Sanna, Telle, and Casargiu. Although dominated by lead and zinc sulfides, the composition of the ore may vary significantly from one vein to another, and sometimes even within the same vein, characterized by banded to brecciated textures. In order of abundance or frequency, the economic minerals at Montevecchio are sphalerite [ZnS], galena [PbS], fahlore [$(\text{Cu}_6[\text{Cu}_4(\text{Fe}, \text{Zn})_2](\text{As}, \text{Sb})_4\text{S}_{13})$], chalcopyrite [CuFeS_2], bournonite [PbCuSbS_3], Ni-Co sulfoarsenides, and pyrite [FeS_2]. The nature of

the minerals forming the gangue is equally variable, they are quartz [SiO₂], barite [BaSO₄], siderite [FeCO₃], Zn carbonate [ZnCO₃], calcite [CaCO₃], ankerite [(Ca,Mg,Mn,Fe)(CO₃)₂], and goethite [FeO(OH)] [24–26].

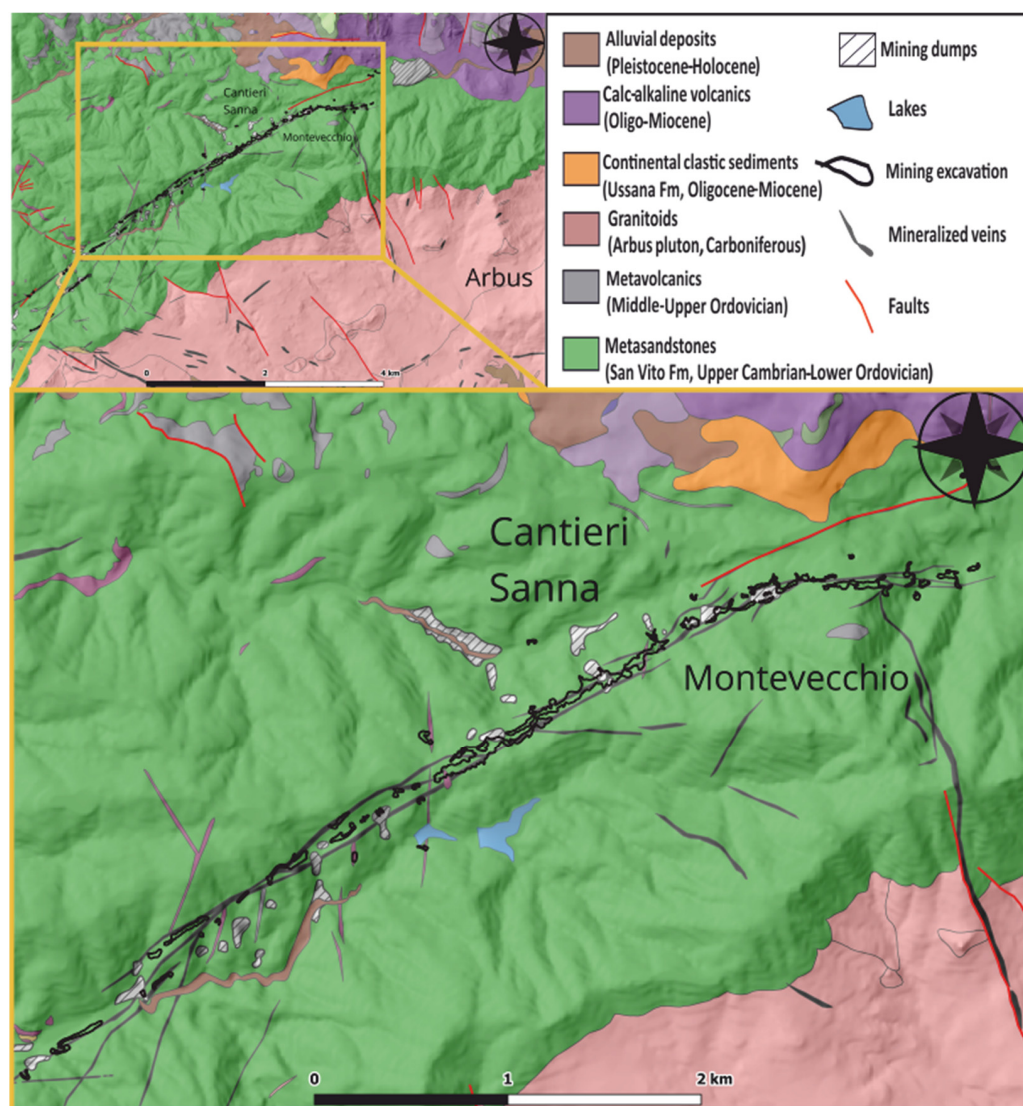


Figure 2. Geological sketch map of the study area.

The Sanna Vein

The Sanna vein was the primary feeder of the Sanna processing plant in Western Montevecchio. The vein displays a smaller longitudinal extension than the other veins of the district (about 300 m), but it has a considerable thickness (15–20 m). A distinctive feature of the Sanna vein is its composition, dominated by supergene minerals. Supergene oxidation processes strongly affected the vein, with an average portion of the oxidated ore reaching about fifty meters in depth and oxidized columnar portions that go down up to 200 m below the topographic surface. The development of supergene processes has deeply transformed the primary sulfide ore (basically: galena, sphalerite, chalcopyrite, and fahlore, with Zn grades of 5–6 wt%, and Pb grades of 1–2 wt%) into secondary phases as anglesite [PbSO₄], cerussite [PbCO₃], iron hydroxides, zinc, and copper secondary minerals (Figure 3). The gangue is mainly sideritic with subordinate quartz; barite may become relatively abundant in the upper parts of the vein; the lead tends to increase at depth while remaining subordinate to zinc [27].

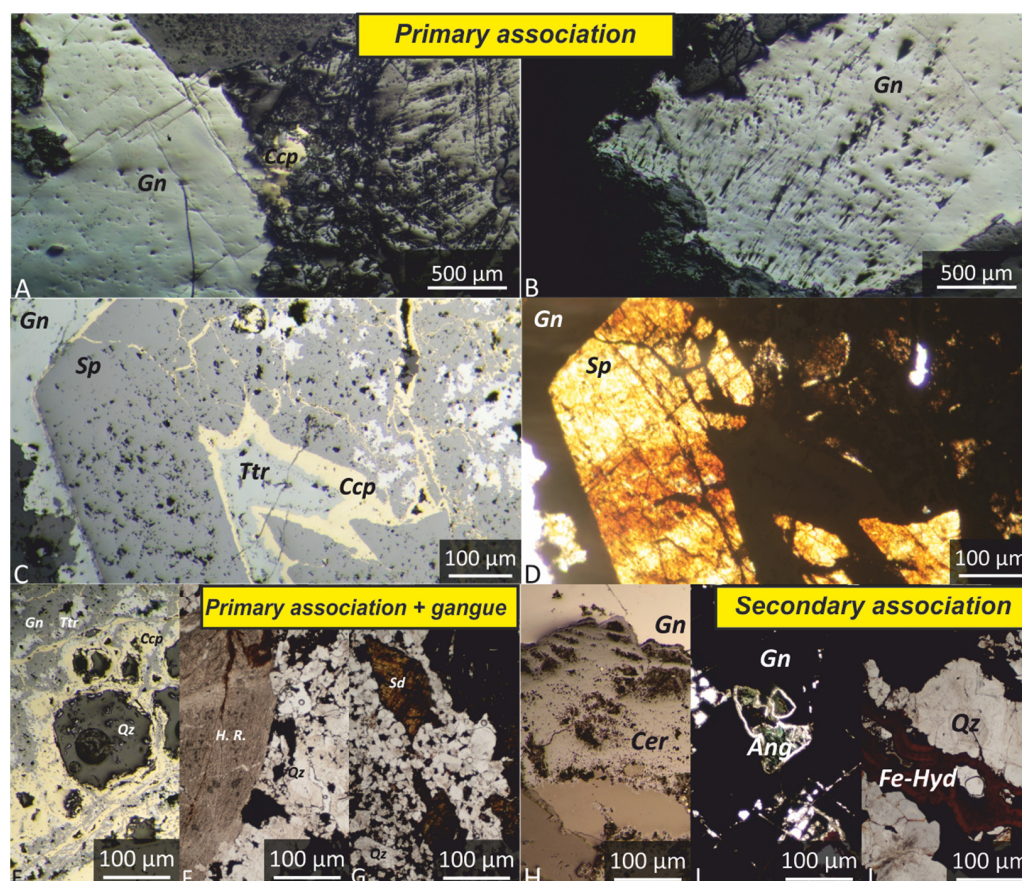


Figure 3. Mineral assemblage of the Sanna vein. (A) Yellow chalcopyrite (Ccp) growing at the edge of galena (Gn). (B) Galena (Gn) brecciated and deformed (as evidenced by the various orientations assumed by the triangular pits), probably grown during a dynamic phase. (C) Tetrahedrite (Ttr) and chalcopyrite (Ccp) included in sphalerite (Sp), in contact with galena (Gn). (D) Sphalerite (Sp) in transmitted light, transparency suggests low iron content. (E) Quartz crystals (Qz), inside galena (Gn), surrounded by chalcopyrite (Ccp) and tetrahedrite (Ttr). (F) Breccia texture with a host rock fragment (H.R.) surrounded by quartz fragments (Qz). (G) Siderite (Sd) crystals surrounded by quartz crystals (Qz) forming a mosaic texture. (H) Cerussite (Cer) aggregate growing on galena (Gn). (I) A crystal of anglesite (Ang) grown within galena (Gn). (J) Iron hydroxides (Fe-Hyd) precipitated between quartz crystals (Qz). (A–C,E,H): plane-polarized reflected light; (D,F,G,I,J): plane-polarized transmitted light. Mineral abbreviations according to Warr (2021) [28].

4. The Sanna Plant Area

The Sanna plant area (about 130,000 m²) is characterized by the remnants of two past mineral processing plants, consisting of tailings, jigging residues, and waste rocks accumulated along the Rio Roia Cani. During mining operations, tailings were discharged as sludge from the treatment plant to the stream, through a drainage tunnel. Initially, sludge was blocked by a series of dams to form tailing ponds. In past mining operations, dams were opened periodically to make space in the ponds. After the mine closure, the main dam collapsed, and the tailings were partially eroded and washed away. Evidence of a consistent solid transport of these materials may be easily traced several kilometres downstream. Currently, the drainage tunnel is damaged, and tailings are affected by rills and gullies that induce instability and small landslides. Tailings preserve the original flat attitude of the pond surface, whilst the jigging wastes form large heaps along the flanks of the valley (Figure 4), quite unstable and incised by surface waters. In the field, tailings and jigging residues are also easily distinguishable by their granulometry; tailings vary from fine sands to clays, while jigging residues vary from gravel to coarse sand. The tailings

cover a surface of about 46.800 m², attaining a thickness of more than 10 m. They display a positive gradation that is interpreted as resulting from sedimentation processes into the tailing pond where the waste materials from the plant were discharged. In addition to the solid transport of the waste materials, evidence of solution transport of elements in the water of the Rio Roia Cani is provided by the frequent occurrence of reddish mineral precipitates and white patinas along the riverbed, particularly where the drainage gallery is broken (Figure 4). The area downstream the Rio Roia Cani is low-populated: main potential targets of contamination are surface- and groundwaters and, in general, the flora and fauna present along the river valley, whose habitat and whose development could be conditioned by the presence of pollutants.

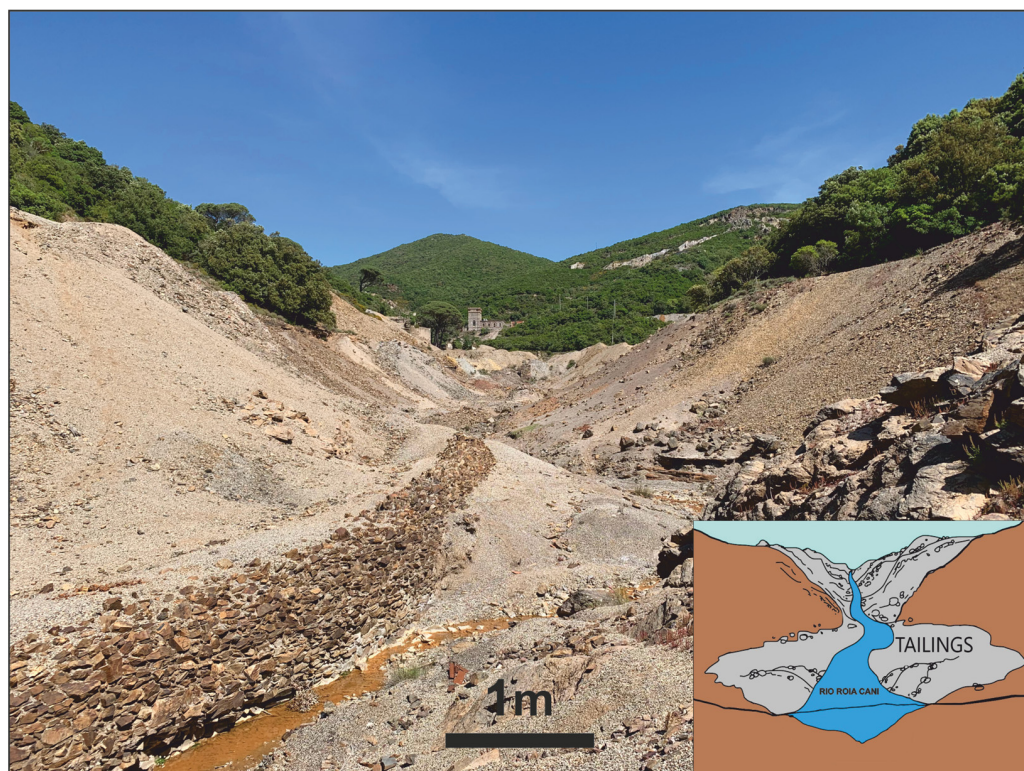


Figure 4. The interaction between the flow of the Rio Roia Cani and the mining wastes.

To complete the environmental frame of this old industrial area, also the mine excavations, located upstream close to the plant area must be considered. They constitute an environment of interaction between surface water and mineralized, potentially polluting rocks. Only part of these waters is now conveyed to the Rio Roia Cani, the great part feeds the groundwater system through the underground mining works.

5. Materials and Methods

5.1. Sampling

Eight samples were collected from the tailings of the Sanna processing plant (Figure 5).

Sampling was carried out following the stratigraphic overlap of different materials, distinguished by chromatic differences and different granulometry (Figure 6).

Nine samples of the white patinas present along the bed of the Rio Roia Cani (Figure 7) were also collected. Sampling was realized paying particular attention to avoid the removal of detrital material present under the patinas.

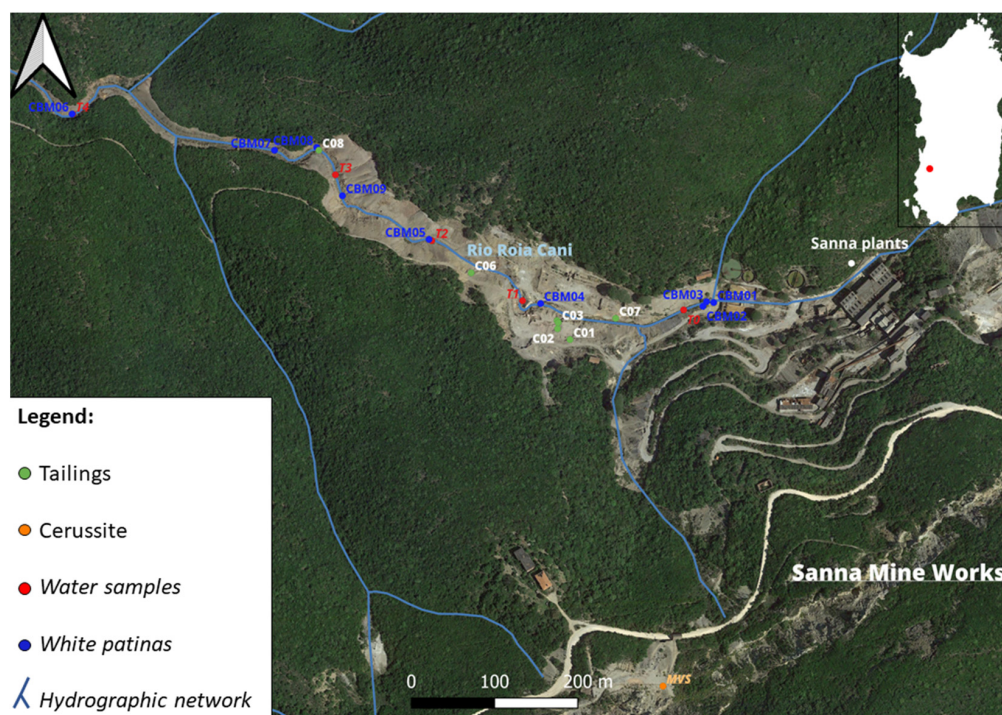


Figure 5. Map with the collected samples. In green, the samples of tailings; in orange, the samples of cerussite; in red, the samples of water; in blue, the samples of white patinas.

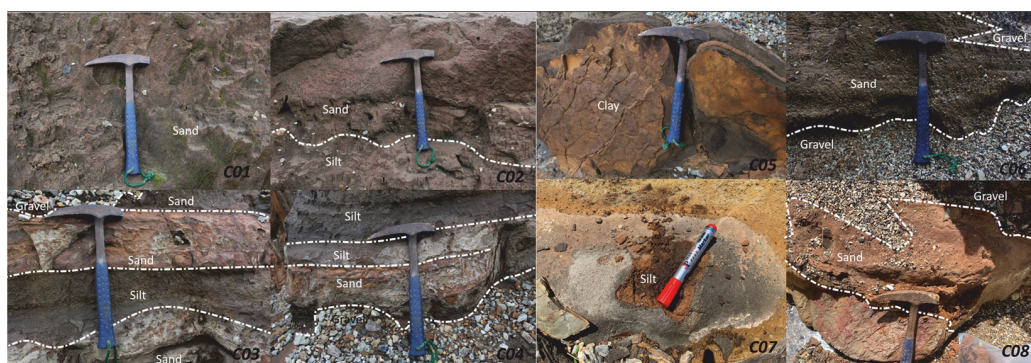


Figure 6. The eight sampled layers of tailings along the Rio Roia Cani.

Some cerussite specimens were collected from the oxidate ore in the mine excavations close to the Sanna plant. Moreover, some water samples were taken on the same day of the white patinas sampling, at different points of the Rio Roia Cani, downstream from the processing plant, to have the same environmental conditions for the two sampling sets (Figure 5).

5.2. X-ray Diffraction Analyses

The eight samples of tailings underwent granulometric analyses at first, then they were analysed by an X-Ray Diffractometer (XRD) to detect the main mineralogical phases. An X'Pert Pro PANalytical diffractometer (Malvern Panalytical, Malvern, UK) with an X-ray tube with Cu anticathode ($\text{Cu-K}\alpha 1 \lambda = 1.54060 \text{ \AA}$), nickel monochromator filter, and X'Celerator detector, was used; data were acquired at 40 kV and 40 mA in an angular range of $5\text{--}70^\circ 2\theta$.



Figure 7. Sampling of the white patinas of the Rio Roia Cani riverbed.

5.3. Scanning Electron Microscope Analyses

The nine samples of white patinas were analysed by XRD, then by Scanning Electron Microscope (SEM) Quanta Fei 200 unit equipped with a ThermoFischer Ultradry EDS detector (Thermo Fischer Scientific, Waltham, MA, USA) operating under low-vacuum conditions, 25–30 KeV voltage, and variable spot size) to study their structure and assess their composition. Samples were not carbon-coated.

5.4. Inductively Coupled Plasma Spectrometry

Chemical analyses of tailings were performed by Inductively Coupled Plasma Mass Spectrometry (ICP-MS, Perkin-Elmer Elan DRC-e, Shelton, CT, USA), after solubilization through acid digestion by aqua regia and hydrofluoric acid, to detect the possible presence of critical materials, metals, and Rare Earth Elements. Eight tailing samples were analysed, together with a certified reference sample (SRM2711), and a blank. Some samples (C04, C07 and C08) were analysed two times, to verify the correctness of the analytical procedures and analyses performed. After acid digestion using aqua regia, cerussite samples were analysed for trace elements by ICP-MS.

White patinas samples were analysed by Inductively Coupled Plasma-Optical Emission Spectroscopy (ICP-OES, Thermo Scientific ARL-3520B Waltham, MA, USA) and ICP-MS, after solubilization by acid digestion by aqua regia and hydrogen peroxide to break down the organic matter component. The water samples were analysed by ICP-MS and by ICP-OES.

6. Analytical Results

Results of the analyses performed on the various types of samples collected on-site are presented below. Samples of tailings were taken in different layers of the old tailing pond, based on chromatic and granulometric variations evidenced in erosional surfaces and gullies along the valley of Rio Roia Cani (Figures 5 and 6). The white patinas were sampled at various points of the riverbed, based on the type of precipitate (Figure 7). The cerussite samples were sampled in the upper part of the Sanna vein, where the primary mineralization was strongly affected by supergene phenomena. The water samples were

collected near some inflows and emergencies, trying to maintain a regular interval between the various sampling points.

6.1. Tailings

Mineralogical analyses (X-ray diffraction) on tailing samples (Figure 8 and Table 1), revealed a composition mainly consisting of host rock and gangue minerals, such as quartz and muscovite (present in all the samples), siderite and barite (found in some samples: C04 and C08 siderite, C03, C04 and C05 barite), and montmorillonite. Primary ore phases are represented by galena and sphalerite. Only one sample (C05) shows the presence of zincite, a secondary phase.

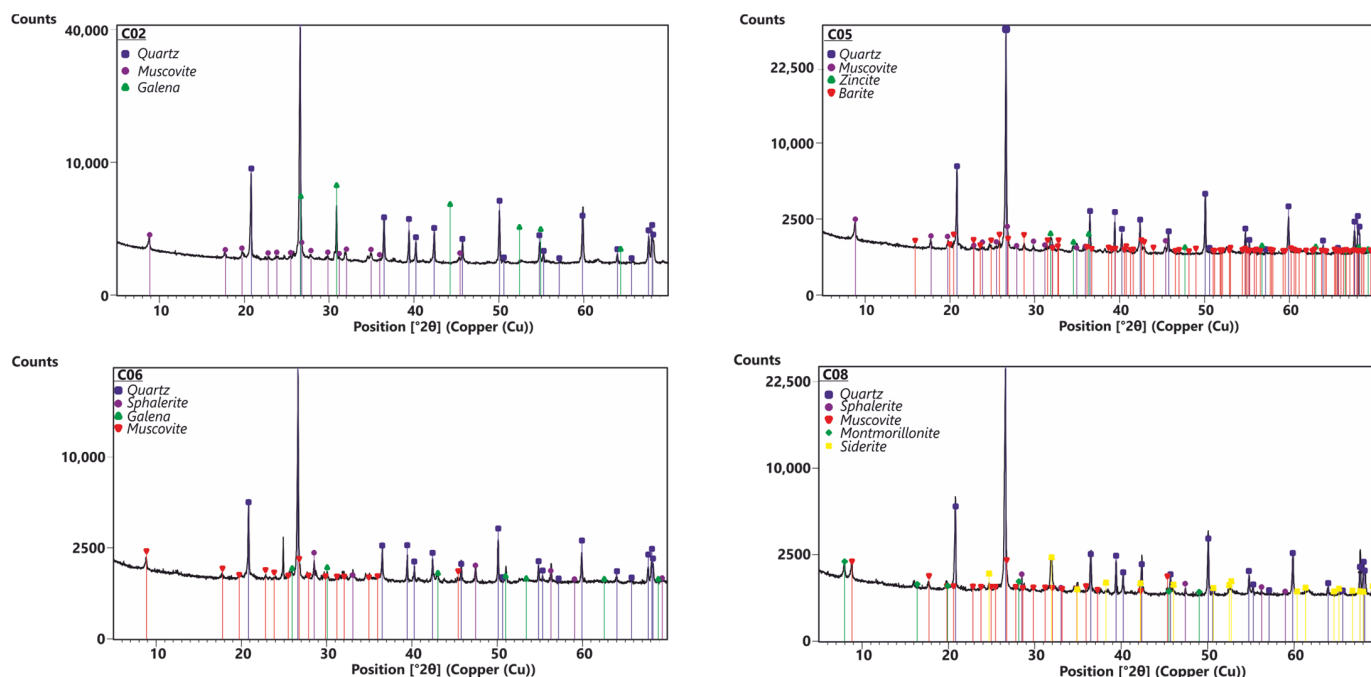


Figure 8. XRD patterns of the mineral phases detected in the different tailing samples. Counts in the y -axis are reported in square root to highlight minor peaks.

Table 1. Summary table of the main characters of sampled tailing layers. Qz = quartz, Ms = muscovite, Dol = Dolomite, Gn = galena, Brt = barite, Sd = siderite, Znc = zincite, Sp = sphalerite, Mnt = montmorillonite. Abbreviation as in [28].

Layer	Approximately Thickness	Sample	Granulometry	Mineralogy
1	50 cm	C01	Moderately graded sand with clays	Qz, Ms, Dol
2	70 cm	C02	Poorly graded sand with clays	Qz, Ms, Gn
3	40 cm	C03	Poorly graded sandy silt with clays	Qz, Ms, Brt
4	50 cm	C04	Poorly graded sand with clays	Qz, Ms, Sd, Brt
5	20 cm	C05	Poorly graded sandy silt with clays	Qz, Ms, Znc, Brt
6	40 cm	C06	Poorly graded gravelly sand with clays	Qz, Ms, Sp, Gn
7	10 cm	C07	Moderately well-graded sand with clays	Qz, Ms
8	50 cm	C08	Poorly graded sandy gravel, with clays	Qz, Ms, Sp, Mnt, Sd

Chemical analyses on the tailing samples show significant amounts of base metals and Rare Earth Elements. A selection of data from the analytical set is reported in Tables 2 and 3. Overall, the dataset displays high Lead and Zinc values, ranging between 760 and 12,300 ppm, and 6600 and 26,500 ppm, respectively. Critical elements once exploited as byproducts in the mine concentrates (Cobalt, Gallium, Indium, Germanium, Antimony,

etc.) show low contents (from 15 to 36 ppm of Co, from 8 to 24 ppm of Ga, from 1 to 13 ppm of In, from 4 to 15 ppm of Ge, from 14 to 170 ppm of Sb). On the other hand, the Rare Earth Elements contents show ranges between 69 and 576 ppm. The highest values are shown by Cerium (26–190 ppm), Lanthanum (10–97 ppm), and Neodymium (11–92 ppm).

Table 2. Analytical data for trace elements in tailings. Values are in mg/kg (ppm).

Sample	Al	As	Ba	Bi	Cd	Co	Cu	Fe	Ga	Ge	In	Mn	Ni	Pb	Sb	Sn	V	W	Zn
C01	19,000	78	1400	ND	47	15	140	61,000	ND	ND	ND	3100	25	2400	28	ND	ND	ND	6800
C02	20,100	55	1200	ND	100	15	110	75,400	10	5	2	4300	35	3000	20	2	27	2	7500
C03	19,000	57	1700	ND	110	22	90	80,200	12	4	2	4500	39	2300	19	3	34	3	8700
C04	17,200	58	2000	ND	70	26	65	93,000	8	4	1	5900	34	760	14	2	21	2	6600
C05	22,700	60	3800	ND	140	25	83	88,200	13	4	2	5800	42	1100	19	3	37	3	11,300
C06	18,700	430	270	5	180	24	2070	135,000	24	15	13	6700	23	12,300	170	10	25	2	26,500
C07	16,700	83	5200	ND	150	36	280	154,000	8	5	2	8000	48	5200	40	2	17	2	15,500
C08	17,200	79	2300	ND	57	15	180	64,600	ND	ND	ND	3300	28	3800	34	ND	31	ND	8700

Table 3. Analytical data for Rare Earth Elements in tailings. Values are in mg/kg (ppm).

Sample	Y	La	Ce	Pr	Nd	Sm	Eu	Gd	Tb	Dy	Ho	Er	Tm	Yb	Lu	ΣREEs + Y
C01	9	12	30	3	12	3	1	3	ND	2	ND	1	ND	1	ND	77
C02	27	45	81	10	38	9	4	10	1	6	1	2	ND	2	ND	236
C03	65	83	180	20	83	22	10	26	4	17	3	6	1	3	ND	523
C04	64	97	180	22	86	23	10	25	3	15	2	5	1	3	ND	536
C05	76	91	190	23	92	26	11	29	4	19	3	6	1	4	1	576
C06	35	73	130	16	65	16	6	17	2	9	1	3	ND	2	ND	375
C07	48	88	140	19	74	19	8	20	3	11	2	4	ND	3	ND	439
C08	8	10	26	3	11	3	1	3	ND	2	ND	1	ND	1	ND	69

In detail (Tables 2 and 3), some elements such as Cu (65–2070 ppm) and Pb (760–12,300 ppm) vary greatly between the various samples, while others, such as As (55–430 ppm), Ba (270–5200 ppm), Cd (47–180 ppm), Fe (64,600–154,000 ppm), Ga (8–24 ppm), Ge (4–15 ppm), In (1–13 ppm), Sb (14–170 ppm), Sn (2–10 ppm), and Zn (6600–26,500 ppm) vary by only one order of magnitude or zero orders of magnitude, such as Al (16,700–22,700 ppm), Co (15–36 ppm), Mn (3100–8000 ppm), Ni (23–48 ppm), V (17–37 ppm), and W (2–3 ppm). Rare Earths Elements show little variability between samples. The C06 sample is particularly enriched in As, Bi, Cd, Cu, Ga, Ge, In, Pb, Sb, Sn, and Zn, the C02 sample shows the highest contents in Al, the C05 in Ba, W, and REEs, and the C07 in Co, Fe, Mn, and Ni. The samples C01 and C08 display the lowest REEs contents.

6.2. The White Patinas

From XRD mineralogical analyses on white patinas, only slight compositional differences between all the samples are found (Figure 9). They are essentially represented by hydrozincite $[\text{Zn}_5(\text{CO}_3)_2(\text{OH})_6]$, except for the CBM03 and CBM05 samples, consisting of zincite $[\text{ZnO}]$.

Based on XRD results, SEM-EDS analyses were performed on the selected CBM01 (hydrozincite) and CBM05 (zincite) representative samples. The morphological study evidenced in the CBM01 sample abundant organic filaments (Figure 10). The EDS spectrum and the EDS compositional maps (Figure 11), show filaments that are made of carbon (C) and oxygen (O). Mineral grains recognizable in the sample are made of zinc (Zn) and oxygen (O), thus confirming the abundance of hydrozincite. Organic filaments are considered to be indicative of biologically mediated formation, as reported for similar occurrences in the same district [18].

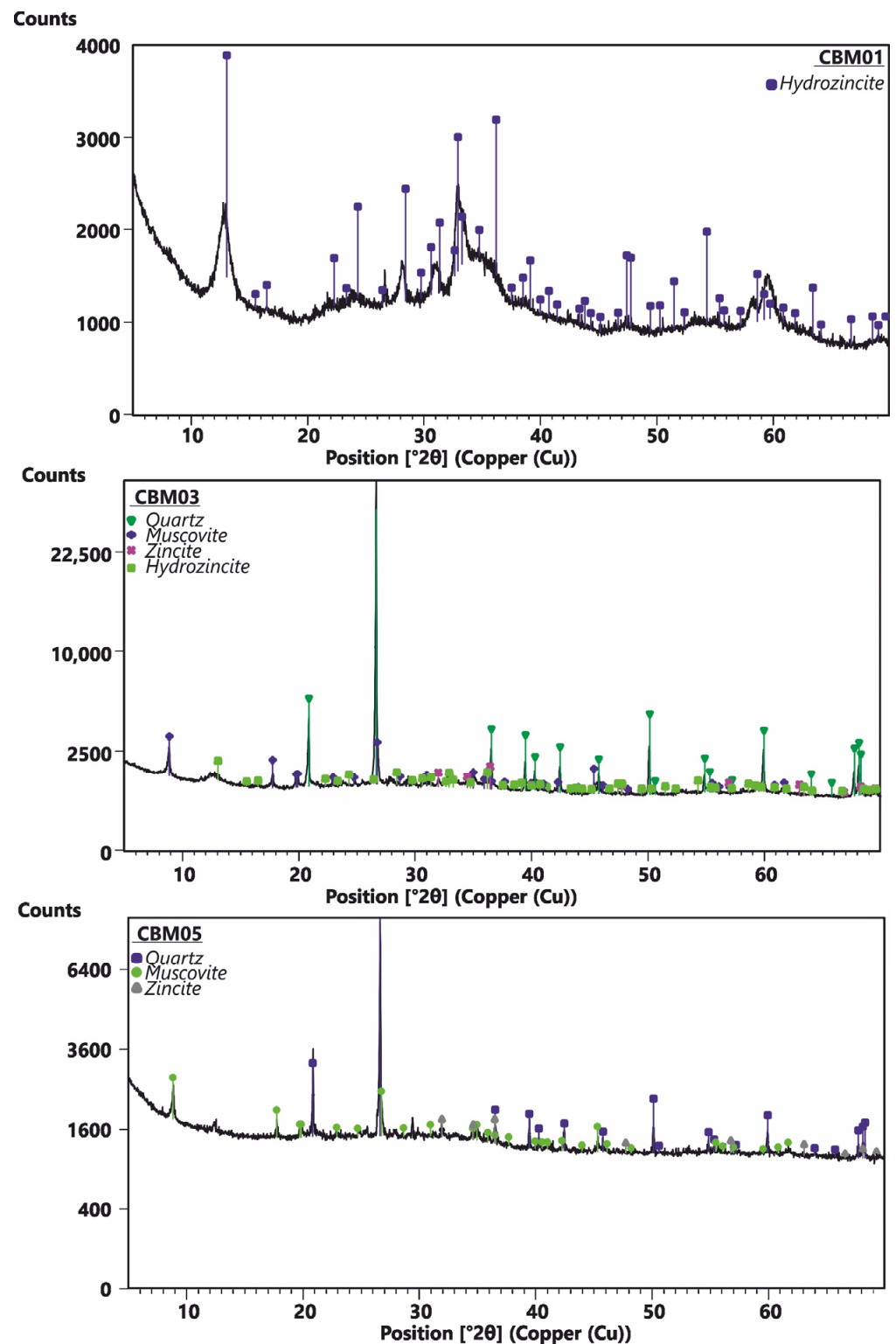


Figure 9. XRD patterns with the mineral phases detected in white patinas. Y-axes report counts in square root to highlight the minor peaks, except the first XRD pattern.

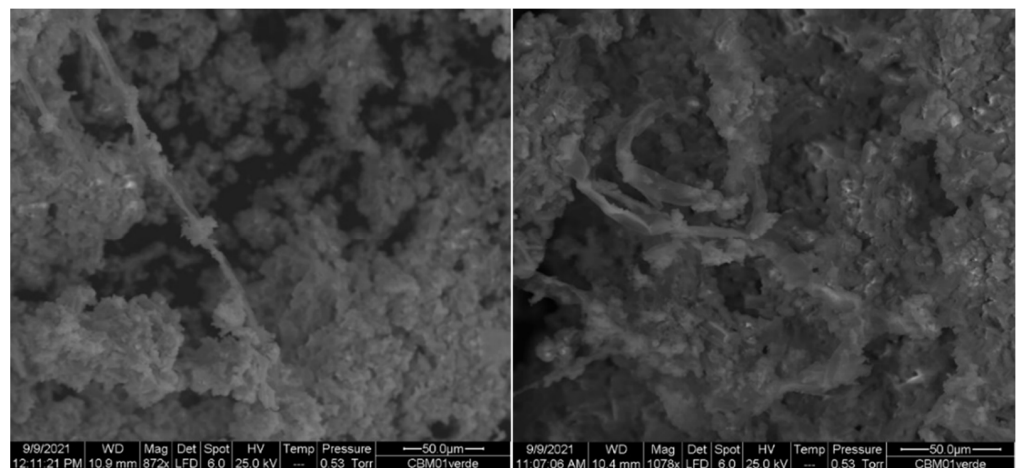


Figure 10. SEM images of CBM01 sample.

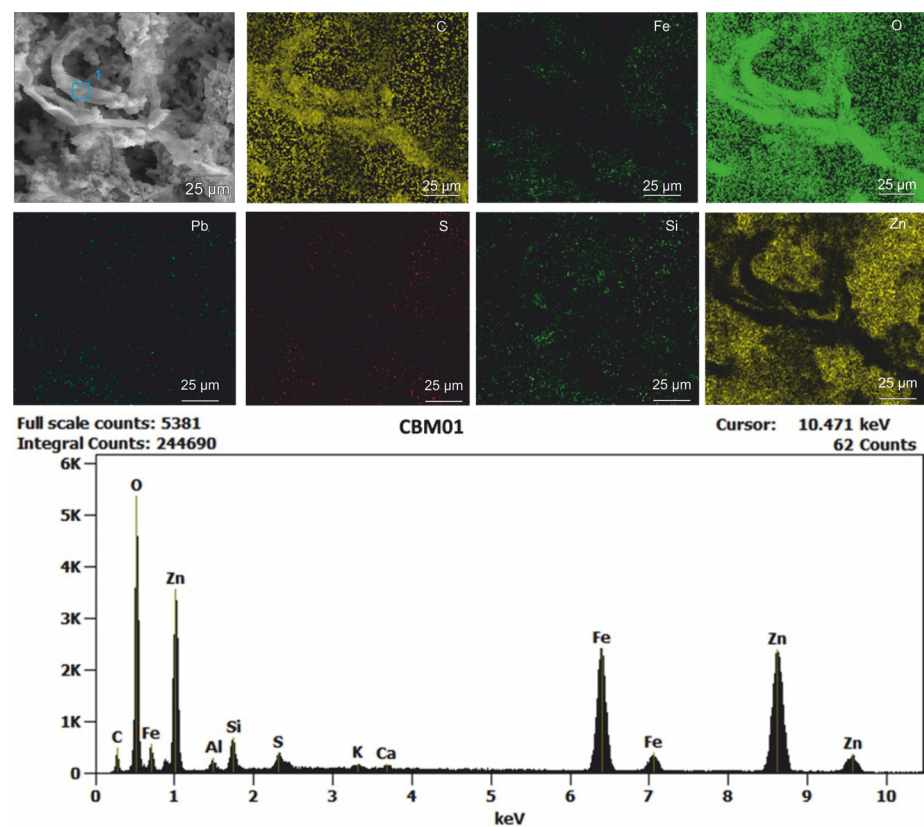


Figure 11. Compositional EDS maps and spectrum for the sample CBM01. The blue square indicates the analysed point.

The CBM05 sample displays a texture dominated by <20 μm elements of globular shape (Figure 12). EDS spectra and compositional maps (Figure 12), confirm the composition reported by the XRD analyses. Moreover, SEM-EDS maps identified grains with traces of arsenic, lead, iron, and oxygen contents, and presence of aluminum-silicates grains.

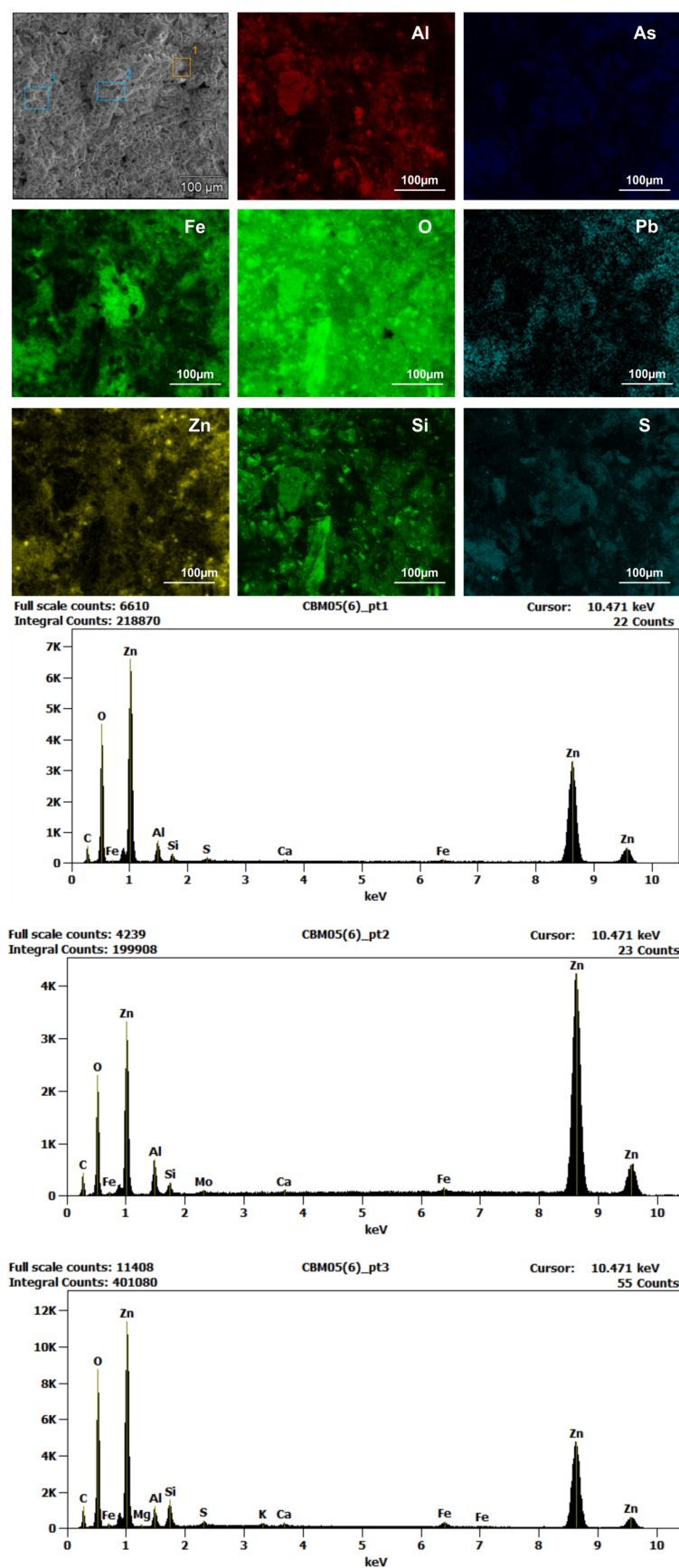


Figure 12. Compositional EDS maps and spectrums for the sample CBM05. The blue and yellow squares indicate the analysed points.

Chemical analyses were performed on each white patinas sample, except for the CBM09, completely utilized for the previous analyses. Trace elements, such as Rare Earth Elements, were analysed by ICP-MS, while major elements were analysed by ICP-OES (Tables 4 and 5).

Table 4. Analytical data for trace elements in white patinas. Values are in mg/kg (ppm).

Sample	Al	As	Ba	Cd	Co	Cu	Fe	Mn	Ni	Pb	Sb	Sr	Zn
CBM01	1770	23	31	610	11	850	27,700	360	150	14,800	8	8	433,200
CBM02	1800	41	310	580	18	730	26,700	650	130	14,600	8	14	415,000
CBM03	10,400	920	16,500	550	84	1430	355,200	14,400	190	33,000	42	200	82,400
CBM04	550	14	120	640	14	300	4870	290	170	6400	5	7	509,000
CBM05	9010	270	1530	400	46	1690	199,800	7450	90	74,500	67	55	90,300
CBM06	10,020	230	11,300	680	29	1490	91,400	4100	92	55,600	110	76	274,300
CBM07	880	23	250	450	10	570	9350	340	130	20,650	13	9	512,200
CBM08	1350	29	860	460	9	660	15,100	400	120	23,370	1	10	489,000

Table 5. Analytical data for Rare Earth Elements in white patinas. Values are in mg/kg (ppm).

Sample	Y	La	Ce	Pr	Nd	Sm	Eu	Gd	Tb	Dy	Ho	Er	Tm	Yb	Lu	ΣREEs + Y
CBM01	250	250	140	61	270	63	24	89	11	45	7	15	1	8	1	1235
CBM02	200	200	110	45	200	44	17	65	8	34	6	12	1	6	1	949
CBM03	250	550	970	120	520	130	52	140	18	72	10	20	2	11	2	2867
CBM04	100	86	38	15	61	13	5	22	3	12	2	5	ND	2	ND	364
CBM05	140	180	280	47	220	56	22	68	8	36	5	11	1	6	1	1081
CBM06	91	140	220	33	140	35	14	40	5	2	3	6	1	3	ND	733
CBM07	84	86	41	13	51	11	4	17	2	9	2	4	ND	2	ND	326
CBM08	100	100	54	17	69	15	6	23	3	13	2	5	ND	2	ND	409

Some elements such as Al (550–10,400 ppm), Ba (31–16,500 ppm), Fe (4870–355,200 ppm), Mn (290–14,400 ppm), Sb (1–110 ppm), and Sr (7–200 ppm), vary by two or three orders of magnitude between the various samples, while others, such as As (14–920 ppm), Cd (400–680 ppm), Co (9–84 ppm), Cu (300–1690 ppm), Ni (90–190 ppm), Pb (6400–74,500 ppm), and Zn (82,400–512,200 ppm) vary by only one order of magnitude. The CBM03 sample is particularly enriched in Al, As, Ba, Co, Fe, Mn, Ni, and Sr, the CBM05 sample is the richest in Cu and Pb, the CBM06 in Cd and Sb, and the CBM07 in Zn.

REEs analyses (Table 5) show little variability among the samples, except for the sample CBM03 which appears to be consistently enriched in REEs (2867 ppm).

6.3. Cerussite

To investigate the origin of the REEs contents found in the tailings of the Sanna plant, a study of supergene mineralization of Sanna vein, which was among the main suppliers of the plant, was performed. An interesting aspect of this mineralization is its predominantly carbonate composition, given that from the most recent literature on Sardinian low-temperature hydrothermal ores [29], high concentrations of REEs are found in carbonate phases. Three samples of cerussite ore, prevalently composed of cerussite and goethite, were collected in the upper part of the Sanna vein (Figure 5). Cerussite crystals were therefore selected from the ore by hand picking, and then analysed by ICP-MS, after acid digestion, to investigate their REEs contents (Table 6).

Table 6. Analytical data for Rare Earth Elements in cerussite. Values are in mg/kg (ppm).

Sample	Y	La	Ce	Pr	Nd	Sm	Eu	Gd	Tb	Dy	Ho	Er	Tm	Yb	Lu	ΣREEs + Y
MVS_1	ND	110	4	ND	120	20	4	6	1	1	ND	ND	ND	ND	ND	266
MVS_2	ND	96	3	ND	100	17	4	5	ND	1	ND	1	ND	ND	ND	227
MVS_3	ND	61	2	ND	64	10	2	3	ND	ND	ND	ND	ND	ND	ND	142

In Table 6 the results of analyses are reported. Lanthanum and Neodymium show the higher values among the REEs.

6.4. Water Analyses

Water samples collected together with the white patinas were analysed by ICP-MS. Overall, water shows a calcium-magnesian sulphate composition [30], characteristic of sulphide mining areas, and amounts of total REEs plus Y of thousands of ng/L (Table 7), several orders of magnitude below the values reported in the literature for mine drainage waters in Montevecchio area [14].

Table 7. Analytical data for Rare Earth Elements in water. Values are in ng/L.

Sample	T [°C]	pH	Eh [mV]	EC [µs/cm]	TDS [mg/L]	Y	La	Ce	Pr	Nd	Sm	Eu	Gd	Tb	Dy	Ho	Er	Tm	Yb	Lu	ΣREEs + Y
T0	16.4	6.3	490	1318	989	1130	730	300	90	340	82	30	130	15	89	17	40	4	19	3	3019
T1	17.5	6.1	491	1301	1071	190	620	750	36	150	34	17	43	4	21	3	5	1	3	ND	1877
T2	16.6	5.7	320	1390	1060	1990	1490	830	240	1040	240	97	400	43	220	35	72	7	45	6	6755
T3	18.6	5.4	471	1365	1030	880	800	290	78	270	64	25	91	10	55	11	22	2	11	1	2610
T4	20.0	4.7	414	1399	1036	450	580	180	57	220	47	25	64	7	34	6	15	1	8	2	1696

From Table 7, the most concentrated REEs in waters are: Y (190–1990 ng/L), La (580–1490 ng/L), Ce (180–830 ng/L), Pr (36–240 ng/L), Nd (150–1040 ng/L), Sm (34–240 ng/L), Gd (43–400 ng/L) and Dy (21–220 ng/L). The sample T0, collected in the stream flow on the tailings immediately downstream to the Sanna processing plant, is among the richest samples in REEs. The sample T1, sampled near a large encrustation of white patina precipitate, is among the poorest samples in REEs. The sample T2 is the richest in REEs, it was sampled where the water leaked off from a collapsed zone of the drainage tunnel of the old tailing pond. The sample T3, among the richest in REEs, was sampled downstream of sample T2. Sample T4, the poorest in REEs, was sampled downstream of other samples and near two tributaries of the Rio Roia Cani (Figure 5).

7. Discussion

Understanding the chemical and mineralogical properties of mining wastes is crucial for the assessment of their economic potential, improving environmental risk assessment, and optimizing the design and execution phases of remediation operations [31]. Raw materials recovery from mining wastes is a specific target for EU policies to improve the supply of CRMs to the Union for the next years [1]. At the same time, these activities provide fundamental contributions to solving environmental issues in abandoned mine areas, as they result in effective remediations of the polluted sites. Effectual recovery of raw materials requires significant technological insight but also requires a strong effort in mineral characterization of waste materials. For the reprocessing of these tailings, it is important to know in detail the initial composition of the ore, the methods used in ore processing, the chemical additives used for mineral beneficiation, how and where tailings were discharged, their current mineralogical composition, and the elements of economic interest contained in them [32]. In environmental studies, tailings characterization generally starts from studies of their granulometry and mineralogy. These characteristics provide essential information on the behaviour of the tailings when they encounter the water [33]. The mineralogy of tailings may change through a single deposit, which may constitute a very heterogeneous system. Minerals in tailings may be very reactive and often soluble in waters under a wide range of environmental conditions; mineralogical characterization of reactive phases (e.g., sulphide and carbonate minerals) allows for predicting the extension and intensity of phenomena such as acid drainage and leaching [31].

7.1. Environmental Issues and Resilience Factors

Several environmental issues emerge from the study in the Sanna plant area. The occurrence in mine wastes, tailings, and secondary precipitates (i.e., the white patinas)

of anomalous geochemical contents of metals (i.e., Fe, Al, Zn, Pb, Mn, Cu, Cd, and Hg) and metalloids (As and Sb), represents a supply of several contaminants having various grades of toxicity that imply different threats for the environment. Depending on the physicochemical conditions of the different interactions of these materials with the Rio Roia Cani waters and with atmospheric agents, it may be produced a prevailing dispersion in solution of metalloids (high-pH interaction), or metals and metalloids (low-pH interaction), followed by diffusion in the environment [34–40]. This chemical transport combines with the solid transport of waste constituents due to high erosion rates in poorly consolidated materials.

X-ray diffraction analyses on the tailings of the Sanna plant identified several metallic minerals which must be regarded as fundamental sources of pollution. Indeed, secondary oxidated phases as zincite are more soluble than sulphides, easily releasing zinc in solution, which is confirmed by the frequent occurrence of hydrozincite/zincite mineral precipitates (white patinas) along the riverbed. The equilibrium between the release of contaminants and their precipitation is influenced by the hydrological regime of the Rio Roia Cani, the temperature, the concentration of metals in the solution, and the Eh-pH conditions.

The co-precipitation of Iron and Lead oxy-hydroxides with zincite, suggested by the red colour of the waters and of the riverbed at the sampling point, is confirmed by SEM-EDS in some white patinas samples (i.e., CBM05 sample), which detected Lead, Iron, and Oxygen. Moreover, precipitation of iron-bearing phases is predicted by saturation calculations (Phreeqc Interactive 3.6.2-15100 software) of the water samples collected along the Rio Roia Cani (Figure 5). Where the T2 water sample was collected, the water was oversaturated in ferrite-Zn and goethite, with saturation indexes of 11.54 and 5.94, respectively.

According to Dore et al., 2020 [41], the microscopic processes that control the dissolution and precipitation of minerals in a polluted mining area may act both positively and negatively towards the environment, favouring the natural abatement or, conversely, the dispersion of pollutants. These microscopic processes may be fundamental for the increase or decrease in metal loads in a river; when positive processes dominate, the load decreases or is limited, but, when negative processes dominate, the load increases, and the dispersion of pollutants can become significant. Overall, metal-enriched precipitates such as white patinas may act as resilience factors in a positive process for the natural environment of the area, removing and fixing relevant amounts of pollutants from the Rio Roia Cani waters. This shows the importance of biologically mediated processes as natural remediation agents, as already observed in the waters of Rio Naracauli [42].

7.2. Raw Materials Potential

Chemical analyses of the Sanna plant tailings (Tables 2 and 3) show that they contain high grades of lead and zinc (up to 1.23 wt% and 2.65 wt%, respectively). The highest Pb grades are attained for sample C06, which is also arsenic and antimony-rich (430 and 170 ppm, respectively), representative of a tailing layer which may have been derived from a fahlore-rich primary ore. Although the materials show generally relatively high contents in total REEs, there is no apparent correlation between the metals present in the highest grades (Pb and Zn) and the REEs. On the other hand, the primary source of REEs in the ore has not yet been discovered; this may lead to the conclusion that the REEs are contained in the gangue and/or in the host rock minerals included in the exploited ore, as reported by Moroni et al., 2019 [20] for the five element-type veins of the southern part of the Montevecchio vein system. The analysed cerussite samples (Table 6) show a slight anomaly in lanthanum and neodymium, indicating a possible role of supergene processes in concentrating these elements in secondary phases. Although the role of weathering processes in REEs mobilization and reconcentration is extensively recognized in lateritic and regolith-hosted, ion-adsorbed-type deposits as well as in weathered carbonatite environments [43,44], REEs behaviour in supergene ore zones of hydrothermal vein deposits is less documented [45].

The white patinas in the Rio Roia Cani are made of Zn-carbonate minerals, thus displaying high Zn contents up to 51.22 wt% (Table 4). Remarkably, they show high contents of REEs (up to 2867 ppm Σ REEs + Y) (Table 5), which display little correlation with Zn and good correlations with As, Fe, and Mn (Figure 13). The zincite samples (CBM03 and CBM05) show the highest values of REEs. A possible role of biological processes in concentrating REEs from waters in the Rio Roia Cani environment can be inferred. Studies on REEs mineralizing processes in exogenic environments evidenced the role of microorganisms in REEs mobilization from primary minerals (phosphates, carbonates, silicates, etc.) to waters, their capabilities in uptaking REEs from waters and fractionating LREEs from HREEs, and to favour and accelerate REEs concentrations in secondary (bio-) minerals [46,47].

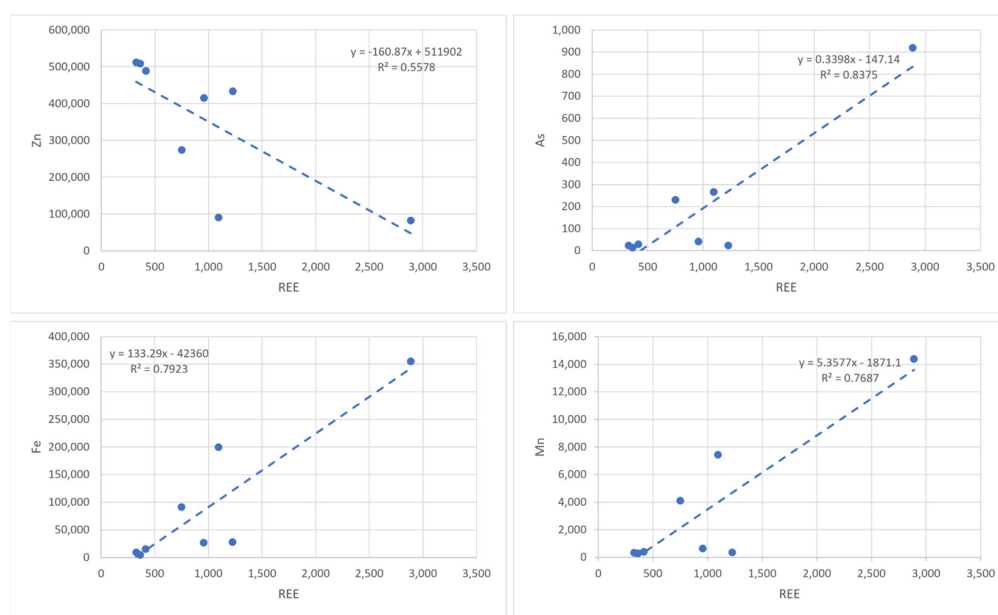


Figure 13. Correlation graphics between some metals and REEs contained in white patinas. Values are in ppm.

The relatively low REEs contents resulting from water analyses of Rio Roia Cani are in good agreement with an effective process of removal of these elements by precipitation of white patinas.

Further insights into the behaviour of REEs in the studied systems are provided by REEs patterns from tailings, white patinas, cerussites and waters, normalized to Post-Archean Australian Shales (PAAS) [48] (Figure 14). Tailings, white patinas, and waters display similar trends: patterns show a flat trend, with a slight enrichment in MREEs and a positive Eu anomaly. They show a good agreement with the patterns reported for the Montevecchio primary ore [6]. Conversely, the cerussite samples show an evident w-type tetrad effect, with strong depletions in Ce, Pr, and HREEs, confirming different paths of REEs fractionation during supergene processes and formation of the secondary ore.

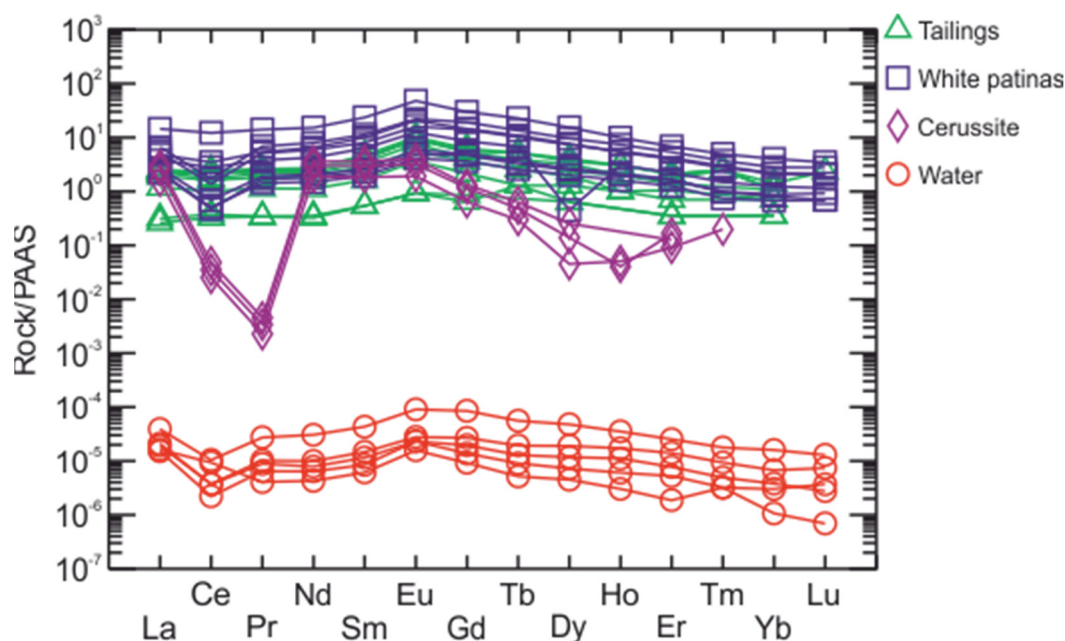


Figure 14. PAAS-normalized REEs patterns for tailings, white patinas, cerussite and waters of the Sanna area.

7.3. Insights for Metals Recovery

Mineral and chemical characterization may also provide some insights into different raw materials recovery from wastes.

The measured contents of Zn and Pb in the tailings may support a project for the recovery of these base metals [49]. In this view, the application of processing techniques essentially depends on different physical (i.e., granulometry) and mineralogical characteristics of waste materials. Due to their fine-grained nature, sulphide-bearing tailings can be effectively treated by flotation, although a large amount of fines increases the consumption of reagents, causing the so-called slime coating phenomenon, hampering the effectiveness of the treatment and, often, making it unfeasible [50]. Successful application of advanced flotation techniques in the processing of the lead and zinc sulphide-bearing tailings of the Principe Tommaso plant in Montevecchio has been recently described in Mercante et al., 2021 [51] and in Sogos et al., 2022 [52]. Different approaches may be required for waste materials in which lead and zinc are contained as oxidate minerals (cerussite, anglesite, smithsonite, hemimorphite, hydrozincite, zincite, etc.), for which metal recovery can be also obtained by leaching techniques (e.g., with sulfuric acid, caustic soda, etc. [53,54]).

The limited presence of economic deposits of REEs and the serious environmental issues related to REE minerals beneficiation [55–59] promoted the studies on alternative and more sustainable treatment techniques, such as biohydrometallurgy, to extract REEs both from primary ores and from secondary resources, as industrial and mining wastes. Recovery of base metals from low-grade ores by bioleaching is a common technique used in the mining industry since the 1970s; it was used with success to leach REEs from mining wastes [60]. As in classical processing techniques, the efficiency of bioleaching is closely linked to the physical and mineralogical composition of the waste materials; actually, the selection of a suitable microorganism depends on the type of REEs minerals (e.g., phosphates, carbonates, etc.) present in the waste, which present different degrees of solubilization in presence of the chemical agents (i.e., organic acids) secreted from microorganisms as chemoheterotrophic bacteria. Biosorption and bioaccumulation processes have been documented for various microorganisms, capable of REEs uptake from leachates [61,62]; conversely, REEs-bearing biomineralization is documented only in a few studies [57,58].

The REEs contents measured in the tailings from the Sanna plant are currently sub-economic, even if with a view to an integral recovery of raw materials from these mine

wastes they must certainly be taken into consideration. The current limited knowledge of Rare-Earth-bearing minerals in the Montevecchio system, however, makes treatment hypotheses for the recovery of these metals premature. Nevertheless, the identification of secondary processes of REEs enrichment in the white patinas constitutes a significant incentive to improve biologically mediated techniques for the recovery of REEs elements from suitable mineral phases. To achieve these goals, the characterization of the REEs mineralogical carriers from primary ore to tailings and the identification of the microorganisms associated with hydrozincite forming the white patinas is of primary importance. Until now, a large part of recent investigations on waste materials in Sardinian mine sites was almost exclusively oriented to the environmental aspects [12–19,41,63]; only a few studies faced the wastes as potential sources of raw materials and CRMs [64–66]. The data acquired in this study allow a series of considerations regarding both the raw material potential and the environmental issues of the Sanna-Rio Roia Cani area.

8. Conclusions

The mineralogical and chemical studies on the tailings of the Sanna processing plant area in Montevecchio confirm that these materials constitute sources of environmental risk. At the same time, they must be regarded as potential economic sources of raw materials, primarily Zinc and Lead. The chemical analyses on the various materials present in the site also highlighted specific layers of REEs-enriched fine-grained products along the stratigraphic sequence of the old tailings pond. The mineralogical carrier of REEs is not yet identified, but an origin from gangue and/or host rock minerals may be reasonably inferred. Some indication of supergene REEs-enrichment of the ore mineralization comes from analyses on cerussite from Sanna mine works. Further evidence of remobilisation processes of REEs in the studied area is provided by the analyses on the white patinas precipitated into the riverbed of the Rio Roia Cani, which display 7.45 wt% of Pb, 51.2 wt% of Zn and about 2900 mg/kg of REEs + Y.

Among the various waste materials present on the site, tailings are confirmed as a primary source of contamination, due to their high contents of pollutants (Pb, Zn, Fe, etc.). Contaminants are transported in solution by rainwater and by the flow of the Rio Roia Cani that erodes the mining dumps. Contamination is partially buffered by white patinas that allow the precipitation of Zn in solution as hydrozincite and zincite, a situation similar to the one currently underway in the Rio Naracauli (Ingurtosu mine, west of Montevecchio), where the riverbed is covered by hydrozincite bio-precipitates [18,63]. Furthermore, the analyses indicate that these white patinas retain other metals, preventing them from remaining in solution and from being dispersed into the environment, generating a sort of remediation process.

This study highlights the presence of CRMs in the tailings, suggesting the possibility of considering these materials as sources of secondary raw materials, as also proposed by recent studies in the Eastern Montevecchio area [66]. REEs found in tailings and white patinas are present in sub-economic to economic values, deserving further studies and insights, for defining their origin, and their processes of mobilisation and concentration in the Rio Roia Cani environment.

Overall, the amount of Zinc, Lead, and CRMs found in the solid matrix led to a hypothesis of evaluation of re-treatment of these solids by various techniques of mineralurgical processing. This re-treatment would entail two benefits: one environmental, through the removal of a primary source of contamination, and the other of an economic nature, through the implementation of a circular economy chain linked to the sale and re-use of these raw materials.

Author Contributions: Conceptualization: L.S., S.N. and G.D.G.; Sampling and field activities: L.S., S.N. and G.D.G.; ICP-MS and ICP-OES analyses: L.S. and F.P.; XRD and SEM-EDS analyses: L.S. and D.F.; Writing-original draft preparation: L.S. and S.N.; Writing, review and editing: L.S., S.N., G.D.G., D.F. and F.P.; Funding acquisition: S.N. and G.D.G. All authors have read and agreed to the published version of the manuscript.

Funding: This paper was produced while attending the PhD course in Earth and Environmental Sciences and Technologies at the University of Cagliari, XXXVIII cycle, with the support of a PNRR scholarship, funded by the European Union, NextGenerationEU, Mission 4 “Education and research” Component 2 “From research to business” Investment 3.1 “Fund for the creation of an integrated system of research and innovation infrastructures”. Title of the PNRR project: GeoSciences IR. Title of the research project: Update of the Sardinian database of mining and mining-metallurgical dumps and identification of their raw material contents, with priority on critical and strategic raw materials for decarbonization and ecological transition. This work was also supported by Fondazione di Sardegna [grant number CUP F75F21001270007] and by the RETURN Extended Partnership, and received funding from the European Union Next-Generati on EU (National Recovery and Resilience Plan—NRRP, Mission 4, Component 2, Investment 1.3—D.D. 1243 2/8/2022, PE0000005).

Data Availability Statement: The data presented in this study are available on request from the corresponding author. The data are not publicly available as they are part of a larger project currently underway for the mapping of Critical Raw Materials in mining wastes at a regional scale.

Acknowledgments: We thank D. Medas, M.L. Deidda, A. Attardi and E. Musu for their support during the sampling and for the suggestions during the development of the final draft of this paper. We acknowledge the CeSAR (Centro Servizi d’Ateneo per la Ricerca) of the University of Cagliari, Italy, for SEM analysis.

Conflicts of Interest: The authors declare no conflict of interest.

References

1. European Commission. Study on the Critical Raw Materials for the EU. Fifth List. Final Report 2023. Available online: <https://op.europa.eu/en/publication-detail/-/publication/57318397-fdd4-11ed-a05c-01aa75ed71a1> (accessed on 20 October 2023).
2. Blengini, G.A.; Mathieux, F.; Mancini, L.; Nyberg, M.; Cavaco Viegas, H.; Salminen, J.; Garbarino, E.; Orveillion, G.; Saveyn, H. *Recovery of Critical and Other Raw Materials from Mining Waste and Landfills*; Publications Office of the European Union: Luxembourg, 2019.
3. Kossoff, D.; Dubbin, W.E.; Alfredsson, M.; Edwards, S.J.; Macklin, M.G.; Hudson-Edwards, K.A. Mine Tailings Dams: Characteristics, Failure, Environmental Impacts, and Remediation. *Appl. Geochem.* **2014**, *51*, 229–245. [\[CrossRef\]](#)
4. Ali, M.A.H.; Mewafy, F.M.; Qian, W.; Alshehri, F.; Almadani, S.; Aldawsri, M.; Aloufi, M.; Saleem, H.A. Mapping Leachate Pathways in Aging Mining Tailings Pond Using Electrical Resistivity Tomography. *Minerals* **2023**, *13*, 1437. [\[CrossRef\]](#)
5. Miler, M.; Bavec, Š.; Gosar, M. The Environmental Impact of Historical Pb-Zn Mining Waste Deposits in Slovenia. *J. Environ. Manag.* **2022**, *308*, 114580. [\[CrossRef\]](#)
6. Moroni, M.; Naitza, S.; Ruggieri, G.; Aquino, A.; Costagliola, P.; De Giudici, G.; Caruso, S.; Ferrari, E.; Fiorentini, M.L.; Lattanzi, P. The Pb-Zn-Ag Vein System at Montevecchio-Ingurtosu, Southwestern Sardinia, Italy: A Summary of Previous Knowledge and New Mineralogical, Fluid Inclusion, and Isotopic Data. *Ore Geol. Rev.* **2019**, *115*, 103194. [\[CrossRef\]](#)
7. Ministero Dell’ambiente e Della Tutela del Territorio. Perimetrazione del Sito di Interesse Nazionale del Sulcis-Iglesiente-Guspinese. GU Serie Generale n. 121 del 27-05-2003. Suppl. Ordinario n. 83. 2003. Available online: <https://www.gazzettaufficiale.it/eli/gu/2003/05/27/121/so/83/sg/pdf> (accessed on 20 October 2023).
8. Progemisa SpA. *Interventi di Bonifica e Ripristino Ambientale Dell’area Mineraria Dismessa di Montevecchio Ponente. Scheda di Intervento di Emergenza E 3.1—Piano di Caratterizzazione*; Public report; Progemisa SpA: Cagliari, Italy, 2003.
9. Sedda, L. *Analisi Ambientale Dell’area di Montevecchio Ponente: Stato Dell’arte E Tecnologie*. Master’s Thesis, Università degli Studi di Cagliari, Cagliari, Italy, 2021.
10. Piano Regionale di Gestione dei Rifiuti. *Piano di Bonifica Siti Inquinati. Schede dei Siti Minerari. Allegato 5*; Regione Autonoma Sardegna: Cagliari, Italy, 2003.
11. *Studio per il Piano di Recupero dell’area Mineraria Dismessa di Montevecchio—Ingurtosu*; Progemisa SpA: Cagliari, Italy, 2001; pp. 190–203.
12. Cidu, R.; Fanfani, L. Overview of the environmental geochemistry of mining districts in southwestern Sardinia, Italy. *Geochem. Explor. Environ. Anal.* **2002**, *2*, 243–251. [\[CrossRef\]](#)
13. Cidu, R.; Frau, F. Impact of the Casargiu Mine Drainage (SW Sardinia, Italy) on the Mediterranean Sea. In Proceedings of the International Mine Water Conference, Pretoria, South Africa, 19–23 October 2009; pp. 926–931.
14. Cidu, R.; Frau, F.; Da Pelo, S. Drainage at Abandoned Mine Sites: Natural Attenuation of Contaminants in Different Seasons. *Mine Water Environ.* **2011**, *30*, 113–126. [\[CrossRef\]](#)
15. Frau, F.; Medas, D.; Da Pelo, S.; Wanty, R.B.; Cidu, R. Environmental Effects on the Aquatic System and Metal Discharge to the Mediterranean Sea from a Near-Neutral Zinc-Ferrous Sulfate Mine Drainage. *Water Air Soil Pollut.* **2015**, *226*, 55. [\[CrossRef\]](#)
16. De Giudici, G.; Medas, D.; Cidu, R.; Lattanzi, P.; Podda, F.; Frau, F.; Rigonat, N.; Pusceddu, C.; Da Pelo, S.; Onnis, P.; et al. Application of hydrologic-tracer techniques to the Casargiu adit and Rio Irvi (SW-Sardinia, Italy): Using enhanced natural attenuation to reduce extreme metal loads. *Appl. Geochem.* **2018**, *96*, 42–54. [\[CrossRef\]](#)

17. De Giudici, G.; Medas, D.; Cidu, R.; Lattanzi, P.; Rignonat, N.; Frau, I.; Podda, F.; Marras, P.A.; Dore, E.; Frau, F.; et al. Assessment of origin and fate of contaminants along mining-affected Rio Montevecchio (SW Sardinia, Italy): A hydrologic-tracer and environmental mineralogy study. *Appl. Geochem.* **2019**, *109*, 104420. [\[CrossRef\]](#)
18. Medas, D.; Lattanzi, P.; Podda, F.; Meneghini, C.; Trapananti, A.; Sprocati, A.; Casu, M.A.; Musu, E.; De Giudici, G. The amorphous Zn biomineralization at Naracauli stream, Sardinia: Electron microscopy and X-ray absorption spectroscopy. *Environ. Sci. Pollut. Res.* **2014**, *21*, 6775–6782. [\[CrossRef\]](#)
19. Podda, F.; Medas, D.; De Giudici, G.; Ryszka, P.; Wolowski, K.; Turnau, K. Zn biomineralization processes and microbial biofilm in a metal-rich stream (Naracauli, Sardinia). *Environ. Sci. Pollut. Res.* **2014**, *21*, 6793–6808. [\[CrossRef\]](#)
20. Cuccuru, S.; Naitza, S.; Secchi, F.; Puccini, A.; Casini, L.; Pavanetto, P.; Linnemann, U.; Hofmann, M.; Oggiano, G. Structural and metallogenic map of late Variscan Arbus Pluton (SW Sardinia, Italy). *J. Maps* **2016**, *12*, 860–865. [\[CrossRef\]](#)
21. Carmignani, L.; Oggiano, G.; Barca, S.; Conti, P.; Salvadori, I.; Eltrudis, A.; Funedda, A.; Pasci, S. *Geologia Della Sardegna: Note Illustrative Della Carta Geologica Della Sardegna in Scala 1:200.000, Memorie Descrittive Della Carta Geologica d'Italia (Vol. 60)*; Servizio Geologico d'Italia: Rome, Italy, 2001; p. 283.
22. Annino, E.; Barca, S.; Costamagna, L.G.; Annino, E.; Barca, S.; Costamagna, L.G. Lineamenti stratigrafico-strutturali dell'Arburese (Sardegna sud-occidentale). *Rend. Semin. Fac. Sci. Univ. Cagliari*. **2016**, *70*, 403–426.
23. Assorgia, A.; Brotzu, P.; Morbidelli, L.; Nicoletti, M.; Traversa, G. Successione e cronologia (K-Ar) degli eventi vulcanici del complesso calco-alcalino oligo-miocenico dell'Arcuentu (Sardegna centro-occidentale). *Period. di Mineral.* **1984**, *53*, 89–102.
24. Salvadori, I. Studio geo-minerario della zona di Salaponi (Sardegna Sud-occidentale). *Boll. Soc. Geol. Ital.* **1958**, *77*, 91–126.
25. Salvadori, I.; Zuffardi, P. Guida per l'escursione a Montevecchio e all'Arcuentu. Itinerari geologici, mineralogici e giacimentologici in Sardegna. *Ente Min. Sardo* **1973**, *1*, 29–44.
26. Moroni, M.; Rossetti, P.; Naitza, S.; Magnani, L.; Ruggieri, G.; Aquino, A.; Tartarotti, P.; Franklin, A.; Ferrari, E.; Castelli, D.; et al. Factors controlling hydrothermal nickel and cobalt mineralization—Some suggestions from historical ore deposits in Italy. *Minerals* **2015**, *9*, 429. [\[CrossRef\]](#)
27. Zuffardi, P. Fenomeni di ricircolazione nel giacimento di Montevecchio e l'evoluzione in profondità della sua mineralizzazione. *Res. Ass. Min. Sarda* **1962**, *1–2*, 17–73.
28. Warr, L.N. IMA–CNMNC approved mineral symbols. *Miner. Mag.* **2021**, *85*, 291–320. [\[CrossRef\]](#)
29. Mondillo, N.; Boni, M.; Balassone, G.; Spoleto, S.; Stellato, F.; Marino, A.; Santoro, L.; Spratt, J. Rare earth elements (REE)—Minerals in the Silius fluorite vein system (Sardinia, Italy). *Ore Geol. Rev.* **2016**, *74*, 211–224. [\[CrossRef\]](#)
30. Corda, V. Studi Sull'impatto Ambientale Delle Discariche Minerarie a Montevecchio Ponente. Master's Thesis, Università degli Studi di Cagliari, Cagliari, Italy, 2022.
31. Jamieson, H.E.; Walker, S.R.; Parsons, M.B. Mineralogical characterization of mine waste. *Appl. Geochem.* **2015**, *57*, 85–105. [\[CrossRef\]](#)
32. Mulenshi, J.; Gilbricht, S.; Chelgani, S.C.; Rosenkranz, J. Systematic characterization of historical tailings for possible remediation and recovery of critical metals and minerals—The Yxsjöberg case. *J. Geochem. Explor.* **2021**, *226*, 106777. [\[CrossRef\]](#)
33. Wang, C.; Harbottle, D.; Liu, Q.; Xu, Z. Current state of fine mineral tailings treatment: A critical review on theory and practice. *Miner. Eng.* **2014**, *58*, 113–131. [\[CrossRef\]](#)
34. Cidu, R.; Caboi, R.; Fanfani, L.; Frau, F. Acid drainage from sulfides hosting gold mineralization (Furtei, Sardinia). *Environ. Geol.* **1997**, *30*, 231–237. [\[CrossRef\]](#)
35. Jurjovec, J.; Ptacek, C.J.; Blowes, D.W. Acid neutralization mechanisms and metal release in mine tailings: A laboratory column experiment. *Geochim. Cosmochim. Acta* **2002**, *66*, 1511–1523. [\[CrossRef\]](#)
36. Frau, F.; Arda, C. Geochemical controls on arsenic distribution in the Baccu Locci stream catchment (Sardinia, Italy) affected by past mining. *Appl. Geochem.* **2003**, *18*, 1373–1386. [\[CrossRef\]](#)
37. Moncur, M.C.; Ptacek, C.J.; Blowes, D.W.; Jambor, J.L. Release, transport and attenuation of metals from an old tailings impoundment. *Appl. Geochem.* **2005**, *20*, 639–659. [\[CrossRef\]](#)
38. Concas, A.; Arda, C.; Cristini, A.; Zuddas, P.; Cao, G. Mobility of heavy metals from tailings to stream waters in a mining activity contaminated site. *Chemosphere* **2006**, *63*, 244–253. [\[CrossRef\]](#)
39. Da Pelo, S.; Musu, E.; Cidu, R.; Frau, F.; Lattanzi, P. Release of toxic elements from rocks and mine wastes at the Furtei gold mine (Sardinia, Italy). *J. Geochem. Explor.* **2009**, *100*, 142–152. [\[CrossRef\]](#)
40. Geng, H.; Wang, F.; Yan, C.; Tian, Z.; Chen, H.; Zhou, B.; Yuan, R.; Yao, J. Leaching behavior of metals from iron tailings under varying pH and low-molecular-weight organic acids. *J. Hazard. Mater.* **2020**, *383*, 121136. [\[CrossRef\]](#)
41. Dore, E.; Fancello, D.; Rignonat, N.; Medas, D.; Cidu, R.; Da Pelo, S.; Frau, F.; Lattanzi, P.; Marras, P.A.; Meneghini, C.; et al. Natural attenuation can lead to environmental resilience in mine environment. *Appl. Geochem.* **2020**, *117*, 104597. [\[CrossRef\]](#)
42. Zuddas, P.; Podda, F. Variations in Physico-Chemical Properties of Water Associated with Bio-Precipitation of Hydrozincite $[Zn_5(CO_3)_2(OH)_6]$ in the Waters of Rio Naracauli, Sardinia (Italy). *Appl. Geochem.* **2005**, *20*, 507–517. [\[CrossRef\]](#)
43. Li, M.Y.H.; Zhou, M.F.; Williams-Jones, A.E. The Genesis of Regolith-Hosted Heavy Rare Earth Element Deposits: Insights from the World-Class Zudong Deposit in Jiangxi Province, South China. *Econ. Geol.* **2019**, *114*, 541–568. [\[CrossRef\]](#)
44. Zhukova, I.A.; Stepanov, A.S.; Jiang, S.Y.; Murphy, D.; Mavrogenes, J.; Allen, C.; Chen, W.; Bottrill, R. Complex REE systematics of carbonatites and weathering products from uniquely rich Mount Weld REE deposit, Western Australia. *Ore Geol. Rev.* **2021**, *139*, Pt B, 104539. [\[CrossRef\]](#)

45. Tuduri, J.; Pourret, O.; Chauvet, A.; Gaouzi, A.; Ennaciri, A. Rare earth elements as proxies of supergene alteration processes from the giant Imiter silver deposit. In Proceedings of the 11th Biennial Meeting SGA, Antofagasta, Chile, 2 June 2014.
46. Li, X.; Liang, X.; He, H.; Li, J.; Ma, L.; Tan, W.; Zhong, Y.; Zhu, J.; Zhou, M.F.; Dong, H. Microorganisms Accelerate REE Mineralization in Supergene Environments. *Appl. Environ. Microbiol.* **2022**, *88*, e0063222. [[CrossRef](#)]
47. Takahashi, Y.; Hirata, T.; Shimizu, H.; Ozaki, T.; Fortin, D. A rare earth element signature of bacteria in natural waters? *Chem. Geol.* **2007**, *244*, 569–583. [[CrossRef](#)]
48. Taylor, S.R.; McLennan, S.M. *The Continental Crust: Its Composition and Evolution*; Blackwell: Oxford, UK, 1985; pp. 1–312.
49. Kaya, M. Assessment of Secondary Zinc and Lead Resources. In *Recycling Technologies for Secondary Zn-Pb Resources*; Kaya, M., Ed.; The Minerals, Metals & Materials Series; Springer: Cham, Switzerland, 2023.
50. Navidi Kashani, A.H.; Rashchi, F. Separation of oxidized zinc minerals from tailings: Influence of flotation reagents. *Miner. Eng.* **2008**, *21*, 967–972. [[CrossRef](#)]
51. Mercante, C. Treatment of Mineral-Metallurgical Residues for the Recovery of Useful. Ph.D. Thesis, Università degli Studi di Cagliari, Cagliari, Italy, 2021.
52. Sogos, G. Study of Mineralurgical Processes for the Treatment of Residues from Mining Activities. Ph.D. Thesis, Università degli Studi di Cagliari, Cagliari, Italy, 2022.
53. Espiari, S.; Rashchi, F.; Sadrnezhaad, S.K. Hydrometallurgical treatment of tailings with high zinc content. *Hydrometallurgy* **2006**, *82*, 54–62. [[CrossRef](#)]
54. Golik, V.; Komashchenko, V.; Morkun, V. Innovative technologies of metal extraction from the ore processing mill tailings and their integrated use. *Metall. Min. Ind.* **2015**, *7*, 49–52.
55. Massari, S.; Ruberti, M. Rare earth elements as critical raw materials: Focus on international markets and future strategies. *Resour. Policy* **2013**, *38*, 36–43. [[CrossRef](#)]
56. Ramos, S.J.; Dinali, G.S.; Oliveira, C.; Martins, G.C.; Moreira, C.G.; Siqueira, J.O.; Guilherme, L.R.G. Rare earth elements in the soil environment. *Curr. Pollut. Rep.* **2016**, *2*, 28–50. [[CrossRef](#)]
57. Cotruvo, J.A. The chemistry of lanthanides in biology: Recent discoveries, emerging principles, and technological applications. *ACS Cent. Sci.* **2019**, *5*, 1496–1506. [[CrossRef](#)] [[PubMed](#)]
58. Castillo, J.; Maleke, M.; Unuofin, J.; Cebekhulu, S. Microbial Recovery of Rare Earth Elements. In *Environmental Technologies to Treat Rare Earth Elements Pollution: Principles and Engineering*; IWA Publishing: London, UK, 2019; Chapter 8; pp. 179–205.
59. Johannesson, K.H.; Zhou, X. Geochemistry of the rare earth elements in natural terrestrial waters: A review of what is currently known. *Chin. J. Geochem.* **1997**, *16*, 20–42. [[CrossRef](#)]
60. Fathollahzadeh, H.; Eksteen, J.J.; Kaksonen, A.H.; Watkin, E.L.J. Role of microorganisms in bioleaching of rare earth elements from primary and secondary resources. *Appl. Microbiol. Biotechnol.* **2019**, *103*, 1043–1057. [[CrossRef](#)] [[PubMed](#)]
61. Park, D.M.; Brewer, A.; Reed, D.W.; Lammers, L.N.; Jiao, Y. Recovery of Rare Earth Elements from Low-Grade Feedstock Leachates Using Engineered Bacteria. *Environ. Sci. Technol.* **2017**, *51*, 13471–13480. [[CrossRef](#)] [[PubMed](#)]
62. Jin, H.; Park, D.M.; Gupta, M.; Brewer, A.W.; Ho, L.; Singer, S.L.; Bourcier, W.L.; Woods, S.; Reed, D.W.; Lammers, L.N.; et al. Techno-economic Assessment for Integrating Biosorption into Rare Earth Recovery Process. *ACS Sustain. Chem. Eng.* **2017**, *5*, 10148–10155. [[CrossRef](#)]
63. De Giudici, G.; Wanty, R.B.; Podda, F.; Kimball, B.A.; Verplanck, P.L.; Lattanzi, P.; Cidu, R.; Medas, D. Quantifying biomineralization of zinc in the rio naracauli (Sardinia, Italy), using a tracer injection and synoptic sampling. *Chem. Geol.* **2014**, *384*, 110–119. [[CrossRef](#)]
64. Buosi, M.; Contini, E.; Enne, R.; Farci, A.; Garbarino, C.; Naitza, S.; Tocco, S. Contributo alla conoscenza dei materiali delle discariche della miniera di Monteponi: I “Fanghi Rossi” dell’elettrolisi, caratterizzazione fisico-geotecnica e chimico-mineralogica, definizione del potenziale inquinante e proposte per possibili interventi. *Res. Ass. Min. Sarda* **1999**, *104*, 49–93.
65. Contini, E.; Naitza, S.; Tocco, S.; Garau, A.; Buosi, M.; Sarritzu, R. Fenomeni di contaminazione da discariche minerarie e metallurgiche nel distretto dell’antimonio del Sarrabus-Gerrei (Sardegna Sud-Orientale): L’area di Su Suergiu-Villasalto. *Res. Ass. Min. Sarda* **2008**, *112*, 45–83.
66. Manca, P.P.; Massacci, G.; Mercante, C. Environmental Management and Metal Recovery: Re-processing of Mining Waste at Montevocchio Site (SW Sardinia). In *Proceedings of the 18th Symposium on Environmental Issues and Waste Management in Energy and Mineral Production: SWEMP 2018*; Widzyk-Capehart, E., Hekmat, A., Singhal, R., Eds.; Springer: Cham, Switzerland, 2019.

Disclaimer/Publisher’s Note: The statements, opinions and data contained in all publications are solely those of the individual author(s) and contributor(s) and not of MDPI and/or the editor(s). MDPI and/or the editor(s) disclaim responsibility for any injury to people or property resulting from any ideas, methods, instructions or products referred to in the content.